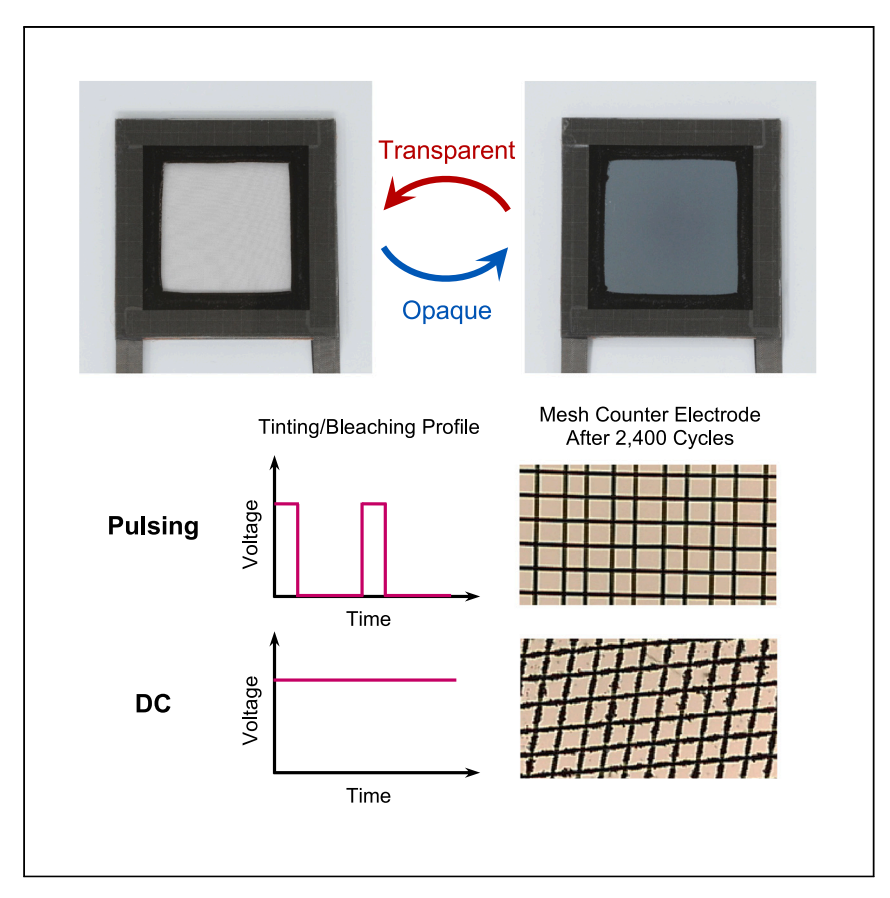


Article

Pulsed electrodeposition for dynamic windows based on reversible metal electrodeposition



Dynamic windows based on reversible metal electrodeposition enable users to electronically control the light into and out of buildings. Herein, Yeang et al. elucidate advantages of pulsing over direct current electroplating for dynamic windows: by effectively suppressing dendrite growth, pulsing enables faster switching to 0.1% transmittance (privacy state) and longer cycle life.

Andrew L. Yeang, Ziliang Li, Sarah Grunsfeld, Gabriel R. McAndrews, Yuchun Cai, Christopher J. Barile, Michael D. McGehee

michael.mcgehee@colorado.edu

Highlights

Pulsed plating suppresses dendrite growth and enables smoother metal films

Metal films tinted using pulsing reach 0.1% transmittance 45% faster than using DC

Pulsed bleaching enables minimal degradation of dynamic windows over 2,400 cycles

Yeang et al., Cell Reports Physical Science 4, 101660

November 15, 2023 © 2023 The Author(s). https://doi.org/10.1016/j.xcrp.2023.101660





Article

Pulsed electrodeposition for dynamic windows based on reversible metal electrodeposition

Andrew L. Yeang,^{1,7} Ziliang Li,^{2,7} Sarah Grunsfeld,³ Gabriel R. McAndrews,⁴ Yuchun Cai,⁵ Christopher J. Barile,⁶ and Michael D. McGehee^{1,2,4,8,*}

SUMMARY

Dynamic windows based on reversible metal electrodeposition electronically tint and bleach, enabling user control of light into and out of buildings. The operating mechanism is to reversibly electrodeposit a thin layer of metal (e.g., Cu and Bi) onto a transparent conductor to block light. Tinting to a desired opacity is constrained by a rough film morphology using direct current (DC) electrodeposition, limiting window switching speed. Here, we show that smoother films can be grown with pulsed electrodeposition with a 10% duty cycle and 1-Hz frequency because ions are able to diffuse past protrusions during the rest phase. While these films initially tint slower compared to DC plating, the films using this pulsing protocol reach 0.1% transmittance 45% faster. Finally, we show that pulsing enables consistent optical properties of dynamic windows after 2,400 cycles due to effective suppression of dendrite growth on the metal mesh counter electrode.

INTRODUCTION

Dynamic windows enable electronic control of light and heat flow into and out of interior spaces, improving both energy efficiency¹ and building aesthetics to improve user experience.^{2,3} Dynamic windows based on reversible metal electrodeposition (RME) are promising due to advantages in color neutrality, cost, and dynamic range compared to conventional electrochromic materials (ion-intercalation^{4–6} and polymers⁷). RME dynamic windows operate by the reversible electrochemical deposition of metal ions (e.g., Bi, Cu, Zn, and Ag) onto a transparent conducting oxide (TCO) working electrode as a metallic film to block light.^{8–14} This process occurs when a reductive potential sufficient for metal plating is applied. As the film grows, the window's transparency decreases (i.e., "tinting" occurs). If the polarity on the electrode is switched, the metal film is oxidized back into the electrolyte, causing the window to "bleach" (i.e., return to its original transparent state). Typically, a mostly invisible metal mesh is used as the counter electrode.^{11–14}

We have previously demonstrated 30 cm \times 30 cm devices with neutral color (C* < 10) that switch from ~65% transmittance to less than 0.1% transmittance in under 10 min¹³ These metrics were achieved by electrode and electrolyte engineering to improve the morphology of the metal deposits to be smooth and compact without degradative reactions (e.g., TCO etching, TCO reduction, or H₂ evolution from the electrolyte) in an aqueous and acidic electrolyte system. ^{12,13}

A common occurrence in metal electrodeposition is to grow protrusions, or "dendrites." For window applications, this dendritic growth is typically undesirable as the metal growing at the tips of the dendrites does not block light, wasting energy and material.^{8,13} In Li battery applications, dendritic growth can also contribute to

¹Department of Chemical and Biological Engineering, University of Colorado Boulder, Boulder, CO 80303, USA

²Renewable and Sustainable Energy Institute, National Renewable Energy Laboratory and University of Colorado Boulder, Boulder, CO 80303, USA

³Department of Mechanical Engineering, University of Colorado Boulder, Boulder, CO 80309. USA

⁴Materials Science and Engineering Program, University of Colorado Boulder, Boulder, CO 80303, USA

⁵Department of Chemistry, University of Colorado Boulder, Boulder, CO 80309, USA

⁶Department of Chemistry, University of Nevada Reno, Reno, NV 89503, USA

⁷These authors contributed equally

⁸Lead contact

*Correspondence: michael.mcgehee@colorado.edu https://doi.org/10.1016/j.xcrp.2023.101660





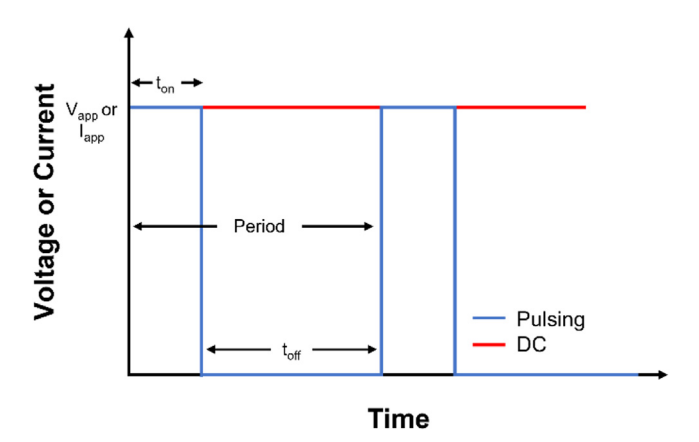


Figure 1. Qualitative schematic for applied voltage or current profiles vs. time for pulsing vs. DC conditions

mechanical failure from "dead" Li and Li pits. 15 Thus, it is desirable in many electrodeposition fields to have smooth and conformal metal films. One way to achieve smooth electrodeposited films is through pulsed electrodeposition. $^{16-20}$

Most electrodeposition occurs using either direct current (DC) plating, whereby a constant current or voltage is held throughout the experiment, or pulsed electrodeposition (pulsing), whereby the current or voltage alternates between two or more values that make up a pulse. Pulsing has been used in metal plating and finishing applications to control deposition morphology, ¹⁶ which in turn controls deposition uniformity and density. ^{17,19,21,22} These pulsed metal finishings are used in a wide range of applications such as trace deposition on circuit boards, corrosion resistant films, ¹⁷ and compositional control of alloys. ^{23,24} Pulsing is typically performed using current control, which controls the rate of reaction. In our electrochemical system, however, we have a relatively strict voltage range in which we operate to ensure metal plating without degradative side reactions, ^{11–13} and thus we have chosen to use voltage control for our electrodeposition for pulsed and direct current.

The simplest version of pulsing has the voltage alternate between a reductive value for metal plating and zero in square waves. There are a few main descriptors for pulsing as shown in Figure 1: applied current or voltage during the "on" pulse, pulse shape (square, triangular, sinusoidal), frequency (or period) of the pulse (Equation 1), and duty cycle (Equation 2).

Frequency =
$$\frac{1}{t_{on} + t_{off}} = \frac{1}{Period}$$
 (Equation 1)

Duty cycle =
$$\frac{t_{on}}{t_{on}+t_{off}} = t_{on} * frequency,$$
 (Equation 2)

where ton and toff represent the on and off time of the pulse.

Figures 2A and 2C show qualitatively the difference in concentration profile between DC and pulsing conditions. The concentration profile grows over plating time in DC conditions following Fick's second law, where the analytical solution of the concentration profile in 1 dimension is shown in Equation 3:

$$C(x,t) = erf\left(\frac{x}{2\sqrt{Dt}}\right),$$
 (Equation 3)



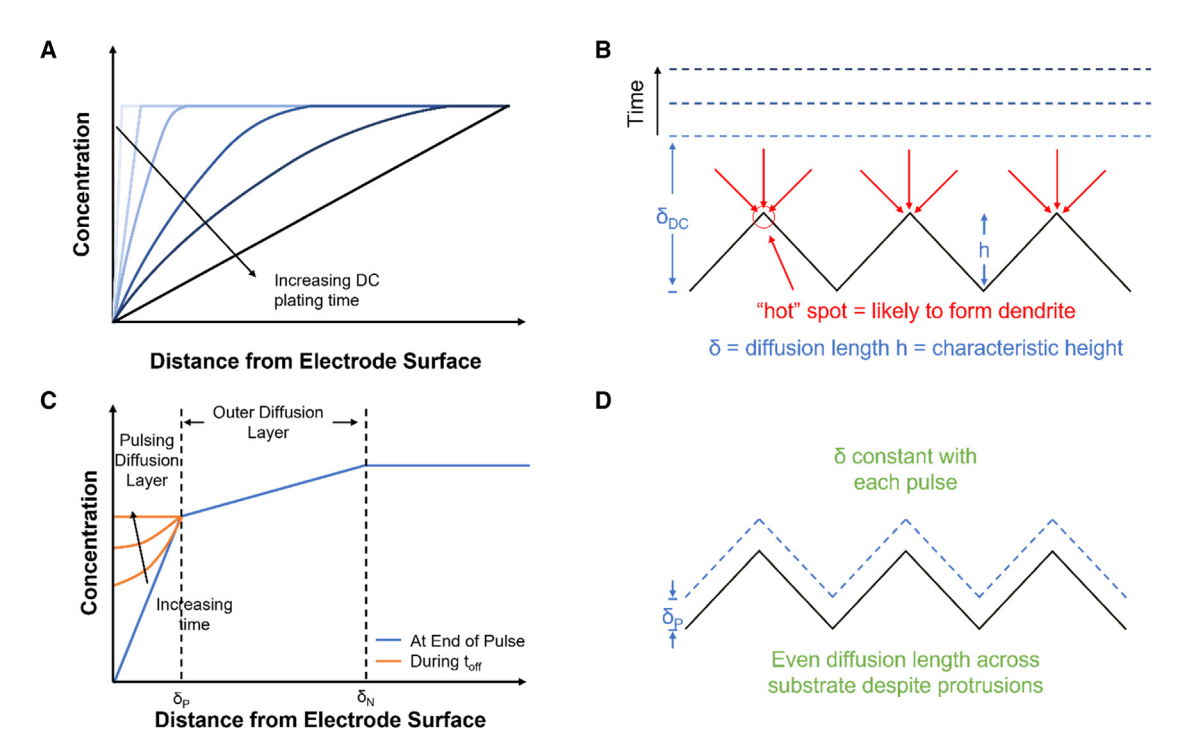


Figure 2. Qualitative schematics for DC and pulsing

(A and C) The concentration profile vs. distance development over plating time for DC conditions (A) and the concentration profile vs. distance development and replenishment over resting time for pulsing (C). 21

(B and D) Schematic showing difference in diffusion length between (B) DC and (D) pulsing conditions during plating and why dendritic features are likely to form in DC plating. Schematics adapted from Ibl. 18

where C is the concentration, x is distance from the electrode surface, D is the diffusion coefficient, and t is time the DC potential has been held. In this case, the diffusion layer (δ_{dc}) will grow with time as shown in Equation 4:

$$\delta_{DC} = \sqrt{\pi Dt}$$
 (Equation 4)

This growth in δ_{dc} means that, if there are local protrusions, metal ions are likely to reach these "hotspots" first and electroplate there, forming a dendrite (Figure 2B). This process is self-reinforcing because the metal ion is likely to plate on this dendrite that protrudes even further from the electrode surface, further growing the characteristic height (h).

The concentration profile, however, for pulsing conditions looks much different. Initially an outer diffusion layer grows, like that of DC conditions, but during the off pulse, the concentration profile can be restored near the electrode surface past any protrusions if $t_{\rm off}$ is sufficiently long, enabling a nearly uniform and consistent concentration profile (and thus plating) for each pulse (Figure 2D). This diffusion length, δ_P , is given by Equation 5:

$$\delta_P = \sqrt{\pi D t_{on}}$$
 (Equation 5)

While Equations 4 and 5 have the same form, δ_{DC} will grow with the deposition time, while δ_P is constant.

In this work, we demonstrate that a pulsed voltage electrodeposition protocol has significant advantages over the previously used DC methods for RME windows. We show that despite tinting faster initially, DC plating takes longer to achieve a



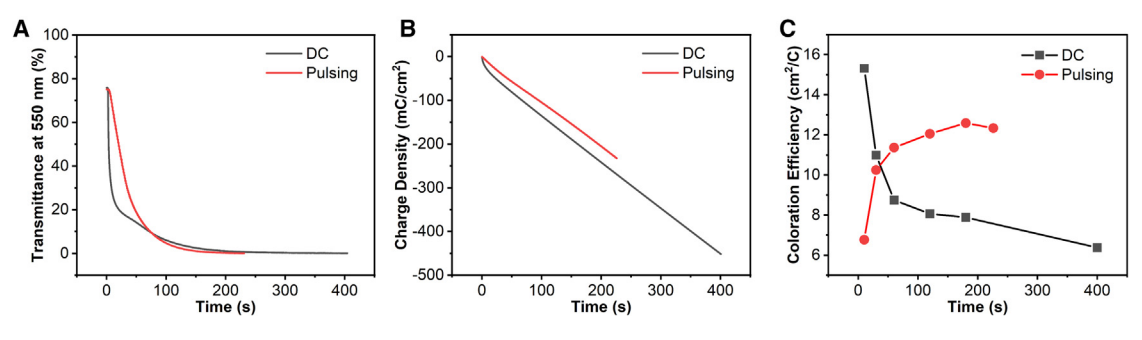


Figure 3. Spectro-electrochemical comparison between DC vs. pulsing onto Pt-ITO

- (A) Transmittance at 550 nm vs. time.
- (B) Charge density vs. time.
- (C) Coloration efficiency at various tinting times.

transmittance state of 0.1% due to a sparse and dendritic film that is less effective at blocking light. In contrast, pulsing results in compact, uniform, and smooth films that are thus more reflective and efficient at blocking light. We realize the benefits of both protocols by implementing a DC step of 10 s before switching to pulsing resulting in a 58% reduction in tinting time to 0.1% transmittance. Finally, we advanced the durability of RME dynamic windows by employing a pulsed voltage cycling profile when stripping the metal from the TCO working electrode and plating it on the metal mesh counter electrode. The pulsing dramatically reduced dendrite growth on the mesh, allowing the windows to maintain consistent optical contrast and coloration efficiency after 2,400 cycles to 10% transmittance.

RESULTS AND DISCUSSION

Spectro-electrochemical characterization

Ibl and Puippe have suggested that the duty cycle for pulsing should be <14% to ensure that the ion concentration profile is restored after each pulse. 20 They also suggest having $t_{\rm on}$ be $\sim\!5x$ the time to charge the double layer $(t_{\rm dl})$ to ensure that the majority of the current contributes to metal plating. We determined $t_{\rm dl}$ to be $\sim\!2.2$ ms for our system by analyzing current vs. time after changing the voltage in a regime where plating does not occur. This analysis is shown in the supplemental information (Figure S1). We performed a matrix of experiments with three duty cycles (10%, 25%, and 50%) and three frequencies (0.1, 1, and 10 Hz) to determine reasonably optimal pulsing conditions and test the theoretical recommendations (Figures S2 and S3). The results led us to choose a 1-Hz frequency and 10% duty cycle for our pulsing conditions. A 10% duty cycle allows the double layer to charge and discharge as well as the concentration profile near the electrode surface to be restored. With a 10% duty cycle, the charge passed is nearly identical for each pulse, which indicates that the region in which the ion density is depleted is not growing as the deposition proceeds (see Note S1 for a more detailed explanation).

When compared to DC electroplating with the same voltage, pulsing tints slower at first but eventually achieves "privacy state" transmittance (0.1% transmittance) both faster and with less charge (Figures 3A and 3B). Coloration efficiency is a metric used to describe how efficiently an electroplated film blocks light, combining the change in optical density and associated charge density passed. Like the transmittance vs. time curves, the coloration efficiency is higher for DC plating initially but is eventually overtaken by pulsing in the later stages of tinting (60 s and beyond, Figure 3C). The lower coloration efficiency for pulsing is likely due to the slow initial tinting and



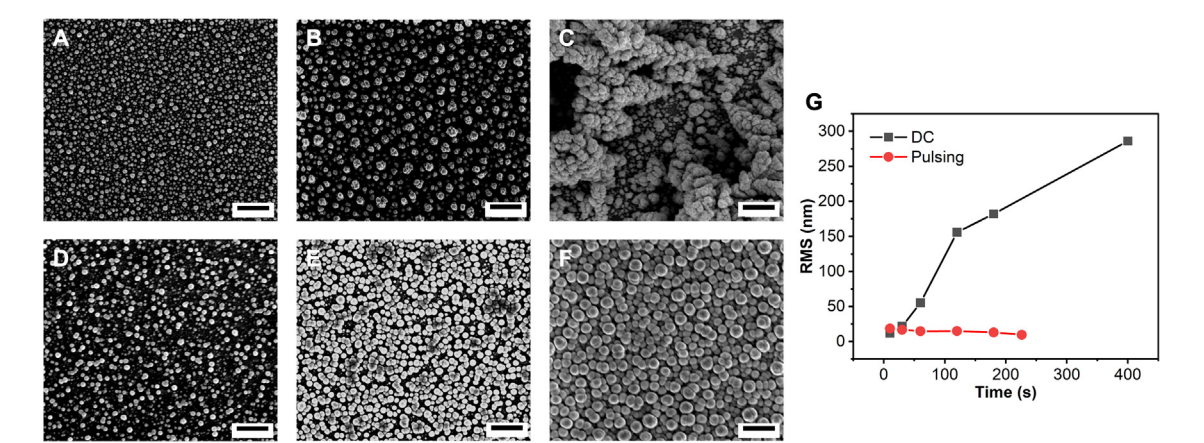


Figure 4. Characterization of the metal films from DC and pulsing conditions

(A–F) SEM images of (A–C) DC conditions (A) after 10 s, (B) after 120 s, and (C) in the 0.1% ("privacy") transmittance state and (D–F) pulsing conditions (D) after 10 pulses, (E) after 120 pulses, and (F) in the privacy transmittance state. Scale bar represents 500 nm.

(G) RMS roughness values obtained with AFM at various tinting states for DC and pulsing conditions. SEM images at more intermediate states and AFM images corresponding to the RMS values are shown in Figures S4–S7.

sparse metal deposits initially compared to DC. As tinting continues, these gaps are filled in more effectively using pulsing, and the metal film is more efficient at blocking light. This phenomenon is further explained in the following section.

Materials characterization

The mechanisms that make pulsing beneficial become clear when looking at the films with scanning electron microscope (SEM) and atomic force microscope (AFM) (Figures 4 and S4-S7) at various stages of plating. In the initial plating when the metal particles nucleate and grow, but do not touch, metal particles from pulsing and DC plating appear similar. The DC-plated films achieve darker tint states faster due to the plating voltage being "on" 100% of the time. As tinting continues during DC plating, the diffusion length for the metal ions in solution grows (Figure 2A), resulting in the growth of metal pillars due to stronger electric fields and shorter diffusion length between the bulk ions and the tips of the pillars (Figure 2B). This dendritic film is less effective at blocking light and requires more metal (and charge) to achieve a given light transmission. In contrast, the diffusion length remains consistent in pulsing as the ion concentration replenishes during the off pulse (Figures 2C and 2D), and the metal ions can more easily diffuse to the electrode surface before being reduced, which creates a more uniform film that is more efficient at blocking light. Figure 4G shows that the root-mean-square (RMS) roughness values obtained with AFM measurements rise to 285 nm with DC plating but stay below 20 nm with pulsed plating. As a result, the thickness of metal needed to achieve privacy state using pulsing is significantly lower when compared to using DC plating (Figure S8).

Optical properties

We measured the reflectance from the metal film side and from the glass side at various tinting states using DC and pulsed plating (Figure 5, see Figure S9 for full spectral data). The reflectance values depend on the direction of incident light as the light interacts with the components in a different order (Figure S10). Overall, the reflectance values are larger for pulsing compared to DC in both orientations. These differences are expected given the SEM (Figures 4A–4F, S4, and S5) and AFM (Figures S6 and S7) images of the films. As we have noted previously, the



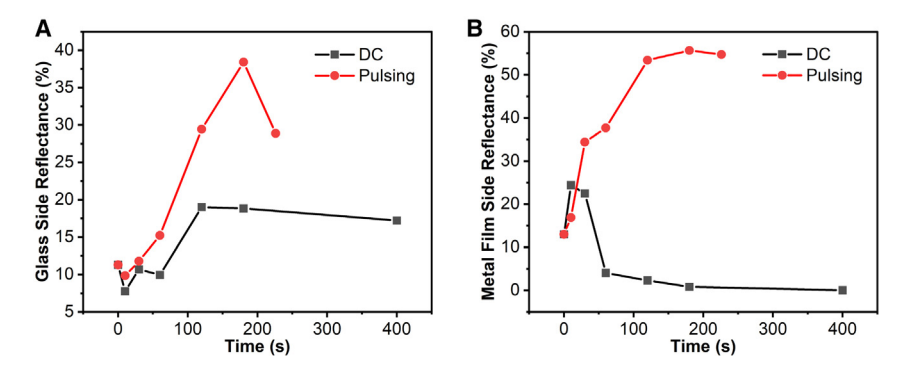


Figure 5. Reflectance at 550 nm of metal films at various tinting times

- (A) Reflectance from the glass side.
- (B) Reflectance from the metal film side.

reflectance is relatively high when light is incident through the glass and TCO because it encounters a smooth continuous metal surface. The reflectance from the other side is significantly more interesting. The metal film-side reflectance increases initially for DC plating before dropping to nearly 0% as the film grows. The reflectivity rises at first because the nucleation is relatively even, and the film is smooth. Eventually, however, the DC metal film becomes rougher and more dendritic, which scatters the light and makes the film absorptive. On the other hand, the reflectance from the metal film side of the pulsing film increases during tinting until it reaches ${\sim}54\%$ and then remains steady with additional plating. This increase in reflectance is expected as the roughness of the film is consistent and smooth throughout plating. The higher reflectivity using pulsing could enable a window to be more effective at reflecting and rejecting heat (Figure S11). 13

Optimized tinting protocol to reduce tinting time by 58%

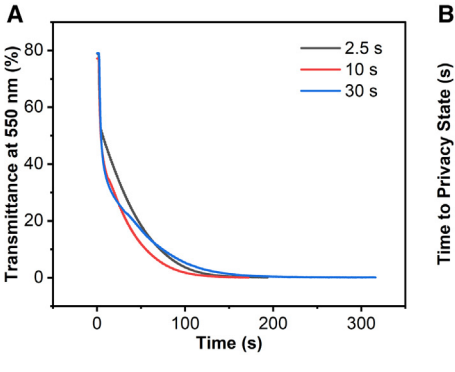
While pulsing ultimately results in faster tinting to privacy state transmittance, DC plating is faster in the initial stages of tinting (Figure 3A). To optimize the tinting protocol to achieve the fastest tinting speed, we explored a protocol using a DC plating step before pulsing (Figures 6A and S12). We observed the optimal DC plating time to be around 10 s (Figure 6B). We attribute this optimization to be at 10 s because in DC plating, the film has not yet achieved a high roughness (Figure 4G), and the concentration profile can still adequately be restored. The optimized protocol reduces the total tinting time to privacy state transmittance by 58% from DC only and 23% from pulsing only. This reduction in tinting time will make these windows substantially more attractive to users.

Pulsing enables longer cycle life

Dendrite growth on the metal mesh counter electrode is a major limiting factor for the cycle life of RME dynamic windows. $^{11-14}$ The avoidance of dendrites through pulsing is thus expected to greatly improve cycle life of the windows. To test the device durability, we fabricated 5 cm \times 5 cm dynamic windows and cycled them to 10% transmittance state (Figure S13). For windows cycled with DC, -0.8 V and +0.8 V was applied to the TCO working electrode during tinting and bleaching, respectively. For windows cycled with pulsing, the voltages applied were kept at the same magnitudes as that for DC cycling with a pulsing frequency and duty cycle of 1 Hz and 10%, respectively. The Cu mesh electrode in the device that cycled with pulsing (i.e., pulsed tinting and pulsed stripping) maintained a smooth surface after 2,400 cycles (Figures 7C and 7D), without significant degradation in optical contrast and coloration efficiency

Article





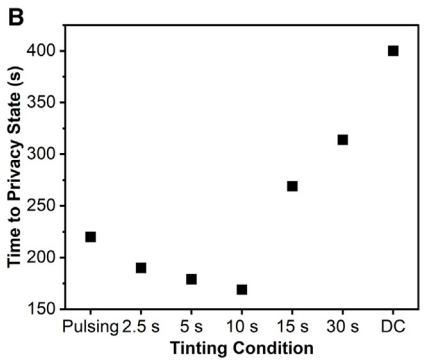


Figure 6. Optimization of tinting protocol

- (A) Transmittance at 550 nm vs. time for various DC times before switching to pulsing.
- (B) Time to privacy state summary using various tinting parameters. Note: data points given with times indicate the amount of time for the DC step before switching to pulsing.

(Figure 8). In contrast, we observed dendrite growth on Cu mesh surrounded with metal debris in the device that cycled with DC after 1,200 cycles (Figure 7A). Dendrites and metal debris continued to develop, leading to significant decay in optical contrast (by 23%) and coloration efficiency (by 39%) after 2,400 cycles (Figures 7B and 8). Note that for both DC and pulsed cycling, 0.1 wt % polyvinyl alcohol (PVA) was added to the electrolyte as a polymer inhibitor to suppress dendrite growth. However, our results indicate that pulsing works synergistically with additives to further suppress dendrite growth and to enhance durability of RME dynamic windows.

We showed that pulsing conditions of 1 Hz and 10% duty cycle enable faster tinting to 0.1% transmittance due to a more dense and uniform film morphology compared to DC conditions despite being slower initially. This film morphology is achieved using pulsing where metal ions can diffuse to the electrode surface during the off pulse. The smooth and uniform morphology enables the metal film to be significantly more reflective. We also showed an optimized protocol that realizes the benefits of faster tinting initially by using a DC step before switching to pulsing, which decreases the tinting time to 0.1% transmittance by 58% compared to the DC-only protocol. Finally, we showed that cycling using pulsing significantly advances device durability: 5 cm × 5 cm RME dynamic windows exhibited consistent optical properties and coloration efficiency over 2,400 cycles. Metal electrodeposition techniques as presented here can be used in various applications to control metal morphology (e.g., in batteries) and to give an additional control to the optical properties of RME dynamic window films (e.g., in thermal camouflage).

EXPERIMENTAL PROCEDURES

Resource availability

Lead contact

Further information and requests for resources should be directed to the lead contact, Michael D. McGehee (michael.mcgehee@colorado.edu).

Materials availability

This study did not generate new unique materials.

Data and code availability

The published article and its supplemental information include all data generated or analyzed during this study.



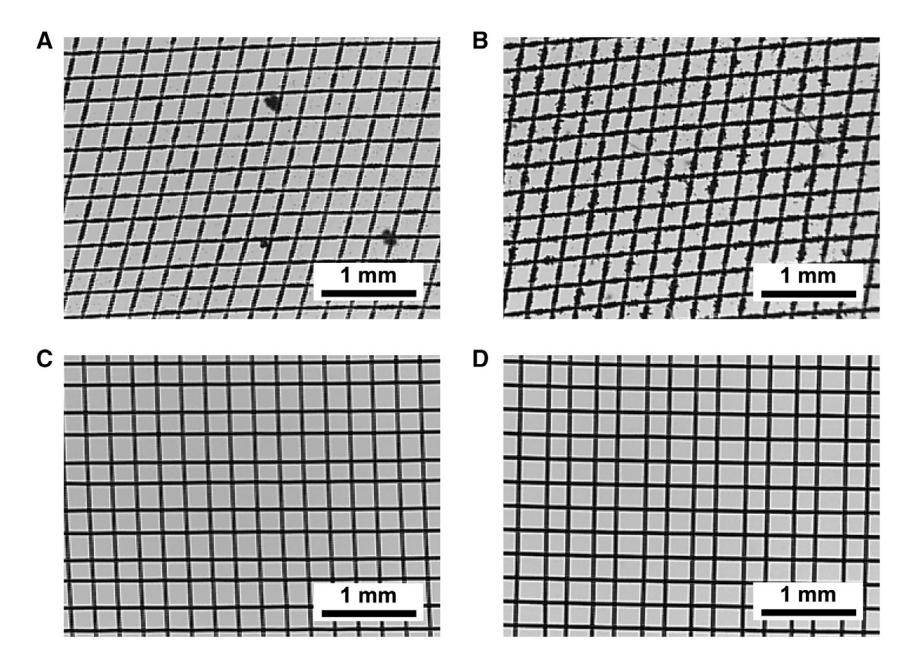


Figure 7. Microscope images of Cu mesh counter electrode of 5 cm \times 5 cm dynamic windows after cycling

(A and B) Cu mesh counter electrode after (A) 1,200 cycles and (B) 2,400 cycles using DC. (C and D) Cu mesh counter electrode after (C) 1,200 cycles and (D) 2,400 cycles using pulsing.

Electrode preparation

Indium tin oxide (ITO) on glass substrates was purchased from Xinyan Technology with glass thickness of 0.7 mm with nominal sheet resistance of 10 Ω \Box^{-1} and was used as the TCO. The TCO substrates were cleaned by sonication in 10 v/v% Extran in DI water solution, DI water, acetone, and then isopropyl alcohol for 15 min each. The substrates were then dried with N $_2$ and cleaned in a UV-ozone cleaner for 15 min. Next, the TCO substrates were placed in a 10 mM 3-mercaptopropionic acid in ethanol solution and placed on a shaker for 24 h. The TCO substrates were then rinsed with ethanol then water before being placed in a Pt-nanoparticle solution (Sigma-Aldrich) diluted 1:19 with DI water and placed on a shaker for 24–72 h. The TCO substrates were then rinsed with DI water, dried with N $_2$, and then annealed at 250°C for 25 min. TCO substrates were treated for 10–15 min in the UV-ozone cleaner prior to use.

Electrolyte preparation

Chemicals were bought and used without purification. The Cu-Bi electrolyte for three-electrode experiments consisted of 10 mM Cu(ClO₄)₂ \cdot 6H₂O (ACROS Organics), 10 mM BiOClO₄ \cdot H₂O (GFS Chemicals), 10 mM HClO₄ (Alfa Aesar) and 1 M LiClO₄ \cdot 3H₂O (ACROS Organics). The electrolyte for two-electrode, 5 cm × 5 cm dynamic windows was the abovementioned electrolyte with 0.1 wt % PVA (M_w = 31,000–50,000, Sigma-Aldrich). PVA was added last and stirred at 1,200 rpm and 70°C until dissolved.

Dynamic window fabrication

Two-electrode, 5 cm \times 5 cm dynamic windows used Pt-modified ITO on glass substrates as the working electrode and Cu mesh (100 mesh, 0.0012" wire diameter) as the counter electrode. Two layers of butyl rubber edge seal (Quanex: Solargain edge tape LP03, 1.5 mm thickness) served as the frame of the dynamic windows.



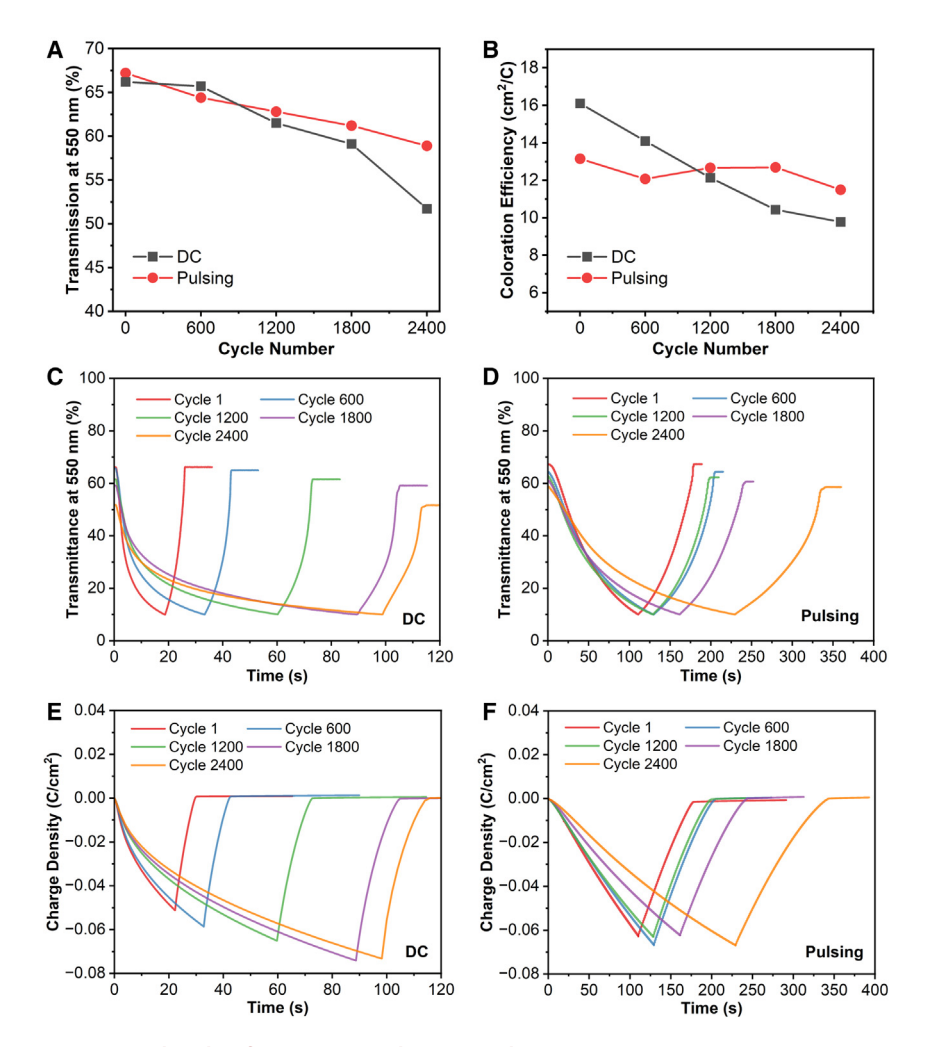


Figure 8. Cycling data for 5 cm \times 5 cm dynamic windows

- (A) Transmittance at 550 nm at clear state after 1, 600, 1,200, 1,800, and 2,400 cycles.
- (B) Coloration efficiency at 550 nm versus number of cycles.
- (C and D) Transmittance at 550 nm for cycle 1, cycle 600, cycle 1,200, cycle 1,800, and cycle 2,400 using (C) DC and (D) pulsing.
- (E and F) Charge density versus time for cycle 1, cycle 600, cycle 1,200, cycle 1,800, and cycle 2,400 using (E) DC and (F) pulsing.

Conductive nylon tape (Conducty Z22, ElectricMosiac) was used to enable electrical contact with the ITO working electrode.

Electrochemical characterization and device cycling

Electrochemical experiments were run using a BioLogic SP-150 potentiostat. Three-electrode experiments used a Pt wire counter electrode and a "no-leak" Ag/AgCl (eDAQ) reference electrode in a glass cuvette (Labomed, G206). Tinting was performed at $-0.7~\rm V$ vs. Ag/AgCl. The immersed geometric surface area of the working electrode was 1.0 cm². Two-electrode dynamic windows were cycled at $-0.8~\rm V$ (DC or pulsing with 1-Hz frequency and 10% duty cycle) until the charge required for cycling was passed for window tinting: 51 mC cm $^{-2}$ for DC and 63 mC cm $^{-2}$ for pulsing for 10% dark state transmission cycling and +0.8 V (DC or pulsing with 1-Hz frequency and 10% duty cycle) until transparency was restored for window bleaching. Check in cycles were run by ensuring 10% transmittance was reached.



Cell Reports Physical Science Article

Characterization

An Ocean Optics OCEAN FX Miniature spectrometer was used in a standard configuration with an Ocean Optics halogen light source (HL-2000) for transmittance and reflectance measurements.

SEM-EDS was run using an FEI Nova 600i HITACHI SU3500 scanning electron microscope operated at an accelerating voltage of 5 kV and equipped with an EDS detector.

SUPPLEMENTAL INFORMATION

Supplemental information can be found online at https://doi.org/10.1016/j.xcrp. 2023.101660.

ACKNOWLEDGMENTS

This research was funded by the National Science Foundation (NSF) under award no. 2127308. This research was supported in part by the Colorado Shared Instrumentation in Nanofabrication and Characterization (COSINC): the COSINC-CHR (Characterization) and/or CONSINC-FAB (Fabrication), College of Engineering & Applied Science, University of Colorado Boulder. The authors would like to acknowledge the support of the staff (Tomoko Borsa) and the facility that have made this work possible.

AUTHOR CONTRIBUTIONS

A.L.Y. and Z.L. contributed equally to this work. A.L.Y.: writing – original draft, writing – review & editing, validation, conceptualization, investigation, and methodology. Z.L.: writing – original draft, writing – review & editing, validation, investigation, and methodology. S.G.: writing – review & editing, validation, investigation, and methodology. G.R.M.: investigation, validation, and writing – review & editing. Y.C.: investigation, validation, methodology, and writing – review & editing. C.J.B.: writing – review & editing, funding acquisition, and supervision. M.D.M.: writing – review & editing, conceptualization, funding acquisition, supervision, and project administration.

DECLARATION OF INTERESTS

M.D.M. is a co-founder of Tynt Technologies, a company commercializing RME dynamic windows. C.J.B. is an advisor to Tynt Technologies. A patent has been filed on the invention described in this manuscript.

INCLUSION AND DIVERSITY

We support inclusive, diverse, and equitable conduct of research.

Received: July 18, 2023 Revised: September 25, 2023 Accepted: October 4, 2023 Published: October 25, 2023

REFERENCES

- View Energy Benefits of View Dynamic Glass in Workplaces. (2015). https://view.com/sites/ default/files/documents/workplace-whitepaper.pdf.
- 2. Hedge, A., and Nou, D. (2018). Ergonomics International Journal Worker Reactions to Electrochromic and Low e Glass Office Windows. Ergon Int J 2, 1–12. https://doi.org/ 10.23880/eoij-16000166.
- 3. Craig, C., and Gregorio, M. (2018). Natural Light Is the Best Medicine for the Office. https://www.prnewswire.com/news-releases/study-natural-light-is-the-best-medicine-for-the-office-300590905.html.
- Granqvist, C.G. (2012). Oxide electrochromics: An introduction to devices and materials. Sol. Energy Mater. Sol. Cell. 99, 1–13. https://doi. org/10.1016/j.solmat.2011.08.021.
- Granqvist, C.G., Arvizu, M.A., Bayrak Pehlivan, İ., Qu, H.-Y., Wen, R.-T., and Niklasson, G.A. (2018). Electrochromic materials and devices for energy efficiency and human comfort in buildings: A critical review. Electrochim. Acta 259, 1170–1182. https://doi.org/10.1016/J. ELECTACTA.2017.11.169.
- 6. Thakur, V.K., Ding, G., Ma, J., Lee, P.S., and Lu, X. (2012). Hybrid Materials and Polymer

Article



- Electrolytes for Electrochromic Device Applications. Adv. Mater. 24, 4071–4096. https://doi.org/10.1002/adma.201200213.
- Mortimer, R.J., Dyer, A.L., and Reynolds, J.R. (2006). Electrochromic organic and polymeric materials for display applications. Displays 27, 2–18. https://doi.org/10.1016/j.displa.2005. 03.003.
- Barile, C.J., Slotcavage, D.J., Hou, J., Strand, M.T., Hernandez, T.S., and McGehee, M.D. (2017). Dynamic Windows with Neutral Color, High Contrast, and Excellent Durability Using Reversible Metal Electrodeposition. Joule 1, 133–145. https://doi.org/10.1016/j.joule.2017. 06.001.
- Araki, S., Nakamura, K., Kobayashi, K., Tsuboi, A., and Kobayashi, N. (2012). Electrochemical Optical-Modulation Device with Reversible Transformation Between Transparent, Mirror, and Black. Adv. Mater. 24. OP122–6OP121. https://doi.org/10.1002/adma.201200060.
- Hernandez, T.S., Barile, C.J., Strand, M.T., Dayrit, T.E., Slotcavage, D.J., and McGehee, M.D. (2018). Bistable Black Electrochromic Windows Based on the Reversible Metal Electrodeposition of Bi and Cu. ACS Energy Lett. 3, 104–111. https://doi.org/10.1021/ acsenergylett.7b01072.
- Strand, M.T., Barile, C.J., Hernandez, T.S., Dayrit, T.E., Bertoluzzi, L., Slotcavage, D.J., and McGehee, M.D. (2018). Factors that Determine the Length Scale for Uniform Tinting in Dynamic Windows Based on Reversible Metal Electrodeposition. ACS Energy Lett. 3, 2823– 2828. https://doi.org/10.1021/acsenergylett. 8b01781.
- 12. Hernandez, T.S., Alshurafa, M., Strand, M.T., Yeang, A.L., Danner, M.G., Barile, C.J., and

- McGehee, M.D. (2020). Electrolyte for Improved Durability of Dynamic Windows Based on Reversible Metal Electrodeposition. Joule 4, 1501–1513. https://doi.org/10.1016/JJOULE.2020.05.008.
- Strand, M.T., Hernandez, T.S., Danner, M.G., Yeang, A.L., Jarvey, N., Barile, C.J., and McGehee, M.D. (2021). Polymer inhibitors enable >900 cm2 dynamic windows based on reversible metal electrodeposition with high solar modulation. Nat. Energy 6, 546–554. https://doi.org/10.1038/s41560-021-00816-7.
- Yeang, A.L., Hernandez, T.S., Strand, M.T., Slotcavage, D.J., Abraham, E., Smalyukh, I.I., Barile, C.J., and McGehee, M.D. (2022). Transparent, High-Charge Capacity Metal Mesh Electrode for Reversible Metal Electrodeposition Dynamic Windows with Dark-State Transmission <0.1%. Adv. Energy Mater. 12, 2200854. https://doi.org/10.1002/ aenm.202200854.
- Sanchez, A.J., Kazyak, E., Chen, Y., Chen, K.H., Pattison, E.R., and Dasgupta, N.P. (2020). Plan-View Operando Video Microscopy of Li Metal Anodes: Identifying the Coupled Relationships among Nucleation, Morphology, and Reversibility. ACS Energy Lett. 5, 994–1004. https://doi.org/10.1021/acsenergylett. 0c00215.
- Garcia, G., Ventosa, E., and Schuhmann, W. (2017). Complete Prevention of Dendrite Formation in Zn Metal Anodes by Means of Pulsed Charging Protocols. ACS Appl. Mater. Interfaces 9, 18691–18698. https://doi.org/10. 1021/acsami.7b01705.
- Fuller, L., Martin, J., Ma, Y., King, S., and Sen, S. (2021). Control of Texture and Morphology of Zinc Films through Pulsed Methods from

- Additive-Free Electrolytes. ChemistrySelect 6, 5426–5434. https://doi.org/10.1002/slct. 202101193.
- Ibl, N. (1980). Some theoretical aspects of pulse electrolysis. Surf. Technol. 10, 81–104. https:// doi.org/10.1016/0376-4583(80)90056-4.
- Ibl, N., Puippe, J., and Angerer, H. (1978). Electrocrystallization in Pulse Electrolysis. Surf. Technol. 6, 287–300.
- Puippe, J.C., and IbI, N. (1980). Influence of charge and discharge of electric double layer in pulse plating. J. Appl. Electrochem. 10, 775–784. https://doi.org/10.1007/BF00611281.
- Doğan, F., Uysal, M., Duru, E., Akbulut, H., and Aslan, S. (2020). Pulsed electrodeposition of Ni-B/TiN composites: effect of current density on the structure, mechanical, tribological, and corrosion properties. Journal of Asian Ceramic Societies 8, 1271–1284. https://doi.org/10. 1080/21870764.2020.1840704.
- Despic, A.R., and Popov, K.I. (1971). The effect of pulsating potential on the morphology of metal deposits obtained by mass-transport controlled electrodeposition. J. Appl. Electrochem. 1, 275–278. https://doi.org/10. 1007/RF00688449
- Ruffoni, A., and Landolt, D. (1988). Pulseplating of AuCuCd alloys-I. Experiments under controlled mass transport conditions. Electrochim. Acta 33, 1273–1279. https://doi. org/10.1016/0013-4686(8)80115-4.
- Ruffoni, A., and Landolt, D. (1988). Pulseplating of Au-Cu-Cd alloys-II. Theoretical modelling of alloy composition. Electrochim. Acta 33, 1281–1289. https://doi.org/10.1016/ 0013-4686(88)80116-6.